

3D All Solid-State Ag–Zn Batteries: A Non-Strategic Chemistry to Meet DoD Energy and Power Needs

Hunter O. Ford,¹ Brian L. Chaloux,² Michael W. Swift,³ Christopher A. Klug,² Youngchan Kim,⁴ Jeffrey W. Long,² Michelle D. Johannes,³ Debra R. Rolison,² and Megan B. Sassin²

¹ *NRL-NRC Postdoctoral Associate in the Chemistry Division, U.S. Naval Research Laboratory, Washington, DC 20375 – hunter.ford.ctr@nrl.navy.mil*

² *Chemistry Division, U.S. Naval Research Laboratory, Washington, DC 20375*

³ *American Society for Engineering Education Postdoctoral Fellow, Center for Computational Materials Science, US Naval Research Laboratory, Washington, DC 20375, USA*

⁴ *Materials Science & Technology Division, U.S. Naval Research Laboratory, Washington, DC 20375*

Abstract: Rechargeable silver–zinc batteries, if improved to deliver more than a few tens of cycles, hold promise as next-generation energy-storage devices by offering competitive energy density, inherent safety, supply-chain resilience, and suitability for reconfiguration as a macroscale 3D all solid-state battery (3D SSB). Implementing a 3D SSB design and simultaneously tackling the issue of undesirable Ag migration during battery operation requires developing an anion-conducting solid-state electrolyte (SSE). Here, we assess the ion-transport properties of a series of crosslinked anion-conducting polymeric SSEs based on 4-dimethylaminomethylstyrene (4DMAMS) and divinylbenzene (DVB). By varying the ratio of functional monomer 4DMAMS to crosslinking monomer DVB, an optimal co-polymer SSE composition with high ionic conductivity and mechanical integrity is achieved. The best performing polymer SSE has an ionic conductivity of 43 mS cm⁻¹ when fully swelled with water, and 0.02 mS cm⁻¹ when equilibrated in 33 % relative humidity (RH).

Keywords: silver–zinc battery, solid-state electrolyte, anion conduction, 3D all solid-state battery

Introduction

Meeting the future energy-storage needs of the civilian market and for defense applications requires battery chemistries that are safer, supply-chain resilient, and more energy dense than lithium-based batteries. A battery chemistry of the past, alkaline silver–zinc (Ag–Zn), is well suited to meet the above requirements.

Silver–zinc batteries are in use as primary cells and as limited secondary batteries, spanning applications across civilian, defense air and naval operations, and NASA systems. The long-term rechargeability of Ag–Zn has been historically prevented by a number of factors, including shape change at the Zn electrode (e.g., Zn dendrites) and dissolution of Ag during cell cycling.^{1,2}

With the invention of a three-dimensional (3D) interconnected and electronically wired Zn anode pioneered by the Naval Research Laboratory, the shape-change and subsequent dendritic shorting of the Zn electrode has been abated.² Further, the door to an interconnected energy-dense 3D Ag–Zn SSB form factor, in which the 3D NRL-patented Zn sponge serves as both anode and scaffold, has been opened. The remaining challenge is the development of an SSE that supports Ag–Zn redox, is amenable to incorporation into the 3D Zn sponge scaffold, and prevents unwanted Ag dissolution and ion-crossover through the cell.

We use *initiated* chemical vapor deposition (*i*CVD) to generate thin, conformal, and anion-conductive polymers that can uniformly coat 2D and complex 3D substrates. The polymers synthesized via *i*CVD are chemically identical to the same polymers synthesized by conventional bulk polymerization methods.³ This chemical comparability means that in tandem with the development of thin *i*CVD anion-conducting SSE coatings for 3D Ag–Zn SSBs, traditional bulk polymerization methods can be used to survey the variable space of polymer SSE composition. In doing so, property–performance relationships regarding the influence of polymer composition

on ion transport and mechanical properties can be rapidly screened. The findings are then translated back to thin *i*CVD-based polymer SSEs en route to a 3D Ag–Zn SSB.

Here, a series of copolymers consisting of DMAMS (dimethylaminomethylstyrene) and crosslinking agent DVB (divinylbenzene) are synthesized via bulk free-radical polymerization and then converted into charged anion-conducting SSEs via post-synthesis solution-based protocols. The influence of polymer composition (ratio of DVB to DMAMS) and impact of water content on ionic conductivity is quantified with electrochemical impedance spectroscopy (EIS), while the mechanical properties are qualitatively assessed. The more highly crosslinked polymers have lower ionic conductivity (σ_i) and a faster drop-off in σ_i as water content decreases, relative to polymers with lower DVB content. The most conductive co-polymer exhibits a σ_i of 43 mS cm⁻¹ when fully swelled with water and 0.02 mS cm⁻¹ at 33% relative humidity.

Experimental

Synthesis of 4-DMAMS monomer: The 4-dimethylaminomethylstyrene (DMAMS) was synthesized according to our recent publication by reacting 1-(chloromethyl)-4-vinylbenzene (Oakwood Products, 98%) with a 5-fold molar excess of dimethylamine (Thermo Fisher, 40% wt/wt aqueous solution) and 1 equivalent K₂CO₃ for 16 hours at 25 °C. The crude product was isolated by aqueous workup (EtOAc/H₂O) and subsequently purified by vacuum distillation (~80 °C, ~200 mTorr). Isolated yields of 75–85% are typical.⁴

Synthesis of DVB-co-DMAMS polymers: As-synthesized DMAMS and commercial DVB (Aldrich, 80% technical grade) were separately passed through short columns of basic alumina to remove inhibitors. For a typical 0.3 g total scale, an appropriate amount of DMAMS was combined with 0.0075 g (2.5 wt%) azobisisobutyronitrile (AIBN, Aldrich, 98%) in a vial. This mixture was sparged with N₂ for 10 min. After sparging, DVB was added to the solution and mixed, and the entire solution was pipetted onto a 2.5 cm × 3.8 cm section of Whatman glass fiber (GF) filter paper (GF/C

1822-849) on top of a glass slide. Another glass slide was placed on top of the monomer-soaked GF, and the entire sandwich was heated to 75 °C on a hotplate for 1.5 h. The resulting 500 μm thick polymer-GF composite was rinsed with acetone to remove unreacted species.

Conversion to Solid-State Electrolyte (SSE): The polymer-GF composite was entirely submerged in the methylating agent methyl iodide (MeI, Fisher Scientific, 99%) within a Parafilm-sealed vial for 24 h; the remaining MeI was then allowed to evaporate. The resultant yellow SSE-GF was rinsed three times with acetone, soaked in 1 M KOH aqueous solution for 24 h and then rinsed with deionized water.

Attenuated Total Internal Reflectance (ATR) Fourier-Transform Infrared Spectroscopy: Spectra were collected on a Thermo Scientific Nicolet iS50 with an ATR-IR attachment. Spectra are collected with 32 scans and a resolution of 4 cm⁻¹ and baseline corrected with Thermo Fisher Omnic data-processing software.

Hydration of SSEs: For samples that were exposed to different relative humidity (RH), the SSE-GF sample was first fully dehydrated within a N₂ drybox (< 2% RH). Next, the SSE-GF was placed in a sealed vessel containing aqueous saturated salt solutions, such that the sample was not in contact with the solution, only the water vapor. Relative humidity (RH) values of 33, 53, 75, and 97% were obtained by using saturated solutions of magnesium chloride, magnesium nitrate, sodium chloride, and potassium sulfate, respectively. After 24 h of equilibration, the sample was ready for analysis. Similarly, for samples that were measured in the entirely water-swelled state, the SSE-GF sample was placed in deionized water for 24 h prior to measurement.

Measurement of ionic conductivity: Roughly 1 cm² of a SSE-GF sample was sandwiched between stainless-steel electrodes with sufficient force to ensure good contact to the electrodes. Samples were interrogated with electrochemical impedance spectroscopy (EIS) using a Gamry Instruments Reference 620 potentiostat with an AC voltage of 100 mV (RMS) over a range of 4 MHz to 0.1 Hz. The resulting data (plotted in Nyquist form, $-Z''$ vs. Z') were fit with equivalent circuit models to obtain the ionic

resistance, from which the ionic conductivity was calculated.

Results and Discussion

In our previous work, *i*CVD was used to prepare thin coatings of pDMAMS which were then converted to SSEs via a reaction with 1-bromo-3-chloropropane.³ This reaction simultaneously quaternizes and introduces chemical crosslinks into the pDMAMS films, where the quaternary ammonium groups are bridged by a propyl spacer. While this method of crosslinking improved the mechanical stability of the films and introduces tethered positive charge, it suffers from two drawbacks. First, it is difficult to control the degree of crosslinking and therefore difficult to evaluate composition–property–performance relationships. Second, as the quaternary ammonium groups are linked together, the loss of degrees of freedom likely negatively impacts ion dissociation and mobility.

To address both concerns, co-polymers of crosslinking agent DVB and DMAMS are prepared in known ratios: 25:75, 10:90, 5:10, and 2.5:97.5 wt% DVB:wt% DMAMS. Charge is then introduced to the DVB-DMAMS co-polymer by reacting with MeI. In this composition, DVB provides the chemical crosslinking, leaving the quaternary ammonium groups with maximal degrees of freedom, which should improve ionic conductivity.

The final polymer (styrenic quaternized ammonium groups with DVB crosslinking) is not a novel material, but the synthetic route used here is amenable to *i*CVD processing to produce thin (sub-micron) polymer films that are readily converted to SSEs for a 3D Ag–Zn SSB.^{5,6} Figure 1 shows ATR-FTIR spectra and chemical structures of the individual monomer components and the 2.5:97.5 DVB-DMAMS SSE-GF co-polymer before and after methylation to introduce positive charge functionality.

The co-polymer is insoluble in solvents that dissolve the respective monomers and contains FTIR peaks associated with both DVB and DMAMS, indicating successful copolymerization and crosslinking. As reported previously, methylation eliminates the amine-tethered C–H peaks at 2770 cm^{-1} and 2810 cm^{-1}

with a new peak at 3008 cm^{-1} being formed, assigned to N^+ -tethered C–H.³ A peak at 1613 cm^{-1} is assigned to N^+ –C while the broad peaks at 3430 cm^{-1} , 3220 cm^{-1} , and 1660 cm^{-1} are assigned to sorbed water.^{7,8} These results confirm the successful methylation of the SSEs.

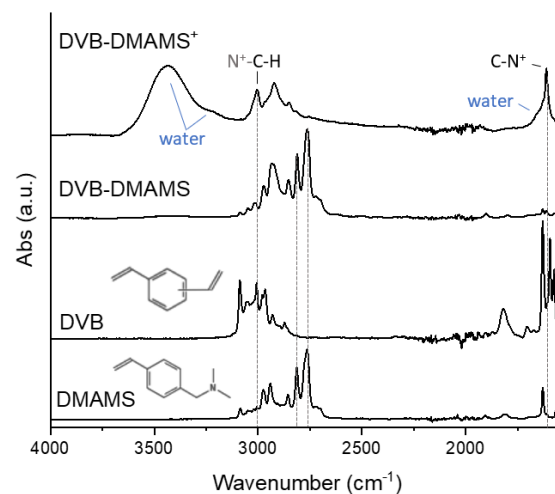


Figure 1. ATR-FTIR spectra of DVB, DMAMS, DVB-DMAMS-GF 2.5:97.5 and DVB-DMAMS⁺-GF 2.5:97.5.

The ionic conductivity values of the four SSE-GF compositions fully swelled with deionized water are shown in Figure 2. The σ_i of the SSE-GF increases as the content of DVB decreases, even when normalized for the number of ion carriers (intrinsic conductivity). The difference is an order of magnitude at the most extreme, with minor differences between 5:95 and 2.5:97.5 compositions. Higher degrees of crosslinking impede ion mobility, likely by disrupting ion transport pathways and preventing significant water uptake into the polymer.^{9,10}

The ionic conductivity of the 5:95 sample is in line with that observed in the literature for a comparable material.⁶ Qualitatively, as the DVB content decreases, the membranes are less rigid and glassy, becoming more rubbery in both the swelled and dried states.

The ionic conductivity of the 2.5 wt% DVB SSE-GF sample equilibrated within different RH environments, along with select RH data of the other membranes, is shown in Figure 3. In the driest condition (2% RH), where the SSE-GF

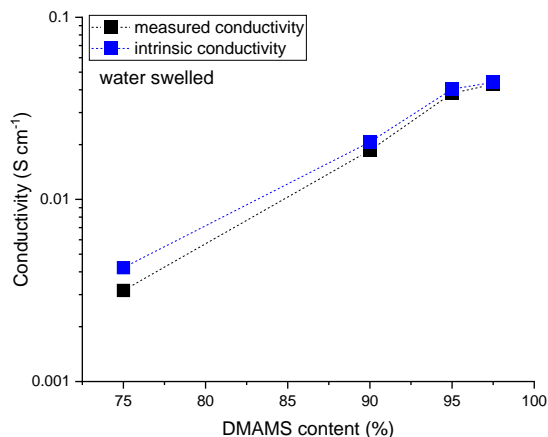


Figure 2. As-measured and intrinsic ionic conductivity of water-swelled SSE-GF samples of varying DMAMS content.

sample was dried in the N₂ dry-box, σ_i is almost immeasurable with EIS, indicating little-to-none of the ion conduction within these materials is done through polymer-ion interactions (such as occurs for Li⁺ conduction in polyethylene oxide) and instead ion conduction is water mediated.

The 2.5 wt% DVB SSE sample maintains reasonably high σ_i at 33% RH (1×10^{-5} S cm⁻¹). The 5:95 and 2.5:97.5 compositions are similar at both points measured. The additional crosslinking content of the 5:95 sample should lead to improved mechanical stability, indicating this composition may have the optimal blend of high ionic conductivity and mechanical strength to serve as an SSE in a 3D Ag-Zn SSB. The more crosslinked compositions of 10:90 and 25:75 exhibit inferior performance at lower RH, experiencing three and four orders of magnitude drops in σ_i , respectively, compared to the two orders of magnitude decrease of the 2.5:97.5 sample when going from fully swelled to 75% RH.

The trends in σ_i seen in Figures 2 and 3 indicate that compositions containing 2.5–5 wt% DVB should be targeted with *i*CVD to yield crosslinked coatings that are mechanically stable with sufficient ionic conductivity, even in low RH environments. Future work will focus on *i*CVD generation of down-selected copolymer

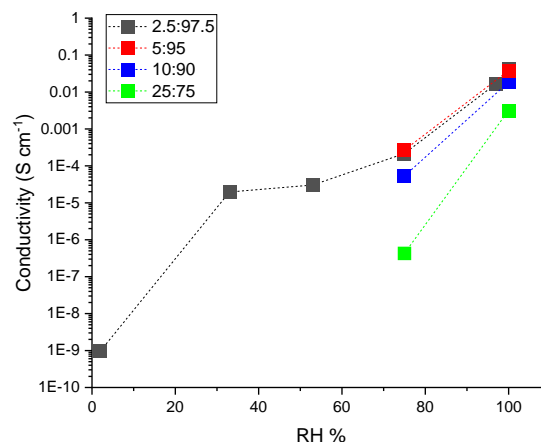


Figure 3. Ionic conductivity of copolymers with varying DMAMS as a function of RH.

compositions, evaluation of Ag and Zn redox reactions, and Ag crossover in 2D and 3D Ag-Zn cells.

Acknowledgements

H. O. F. gratefully acknowledges the National Research Council Postdoctoral Fellowship Program.

References

- Parker, J. F.; DeBlock, R. H.; Hopkins, B. J.; Chervin, C. N.; Rolison, D. R.; Long, J. W.; Sassin, M. B. *J. DoD Res. Eng.* **2022**, *5*, 97–106.
- Parker, J. F.; Chervin, C. N.; Nelson, E. S.; Rolison, D. R.; Long, J. W. *Energy Environ. Sci.* **2014**, *7*(3), 1117–1124.
- Ford, H. O.; Chaloux, B. L.; Rolison, D. R.; Sassin, M. B. *ACS Appl. Mater. Interfaces* **2023**.
- Kim, Y. C.; Chaloux, B. L.; Rolison, D. R.; Sassin, M. B.; Johannes, M. D.; Sassin, M. B. *Electrochem. Commun.* **2022**, *140*, 107334.
- Small, H. *J. Chromatogr. A* **1991**, *546*, 3–15.
- Maurya, S.; Shin, S. H.; Kim, M. K.; Yun, S. H.; Moon, S. H. *J. Membr. Sci.* **2013**, *443*, 28–35.
- Ferrari, M. C.; Catalano, J.; Baschetti, M. G.; De Angelis, M. G.; Sarti, G. C. *Macromolecules* **2012**, *45*(4), 1901–1912.
- Arges, C. G.; Wang, L. H.; Jung, M. S.; Ramani, V. *J. Electrochem. Soc.* **2015**, *162*(7), F686–F693.
- Tsehaye, M. T.; Choi, N. H.; Fischer, P.; Tubke, J.; Planes, E.; Alloin, F.; Iojoiu, C. *ACS Appl. Energy Mater.* **2022**, *5*(6), 7069–7080.
- Maurya, S.; Shin, S. H.; Kim, Y.; Moon, S. H. *RSC Adv.* **2015**, *5*(47), 37206–37230.